Analysis of natural fibre composites for aerospace structures

Analysis of natural fibre composites for aerospace structures

Salvatore Brischetto*

Abstract

- ***Purpose*** **:** *The main idea is the comparison between composites including natural fibres (such as the linoleum fibres) and typical composites including carbon fibres or glass fibres. The comparison is proposed for different structures (plates, cylinders, cylindrical and spherical shells), lamination sequences (cross-ply laminates and sandwiches with composite skins) and thickness ratios. The purpose is to understand if linoleum fibres could be useful for some specific aerospace applications.*
- ***Methodology*** **:** *A general exact three-dimensional shell model is employed for the static analysis of the proposed structures in order to obtain displacements and stresses through the thickness. The shell model is based on a layer-wise approach and the differential equations of equilibrium are solved by means of the exponential matrix method.*
- ***Findings*** **:** *In qualitative terms, composites including linoleum fibres have a mechanical behavior similar to composites including glass or carbon fibres. In terms of stress and displacement values, composites including linoleum fibres can be used in aerospace applications with limited loads. They are comparable with composites including glass fibres. In general, they are not competitive with respect to composites including carbon fibres. Such conclusions have been verified for different structure geometries, lamination sequences and thickness ratios.*
- ***Originality*** **:** *The proposed general exact 3D shell model allows the analysis of different geometries (plates and shells), materials and laminations in a unified manner using the differential equilibrium equations written in general orthogonal curvilinear coordinates. These equations written for spherical shells degenerate in those for cylinders, cylindrical shell panels and plates by means of opportune considerations about the radii of curvature. The proposed shell model allows an exhaustive comparison between different laminated and sandwich composite structures considering the typical zigzag form of displacements and the correct imposition of compatibility conditions for displacements and equilibrium conditions for transverse stresses.*

Keywords: laminates and sandwiches, plates and shells, carbon fibres, glass fibres, linoleum fibres, exact 3D shell model.

*Corresponding author: Salvatore Brischetto, Department of Mechanical and Aerospace Engineering, Politecnico di Torino, corso Duca degli Abruzzi, 24, 10129 Torino, ITALY. tel: +39.011.090.6813, fax: +39.011.090.6899, e.mail: salvatore.brischetto@polito.it.

1 Introduction

The next generation of aircraft and spacecraft could achieve new targets using innovative multilayered configurations for their structural parts (see Brischetto et al. (2016a) and Ferro et al. (2016)). Typical multilayered configurations for aerospace applications are sandwich plates and shells (embedding a soft core and external classical or composite skins) or composite laminates. In these configurations, the most employed materials are Carbon Fibre Reinforced Composites (CFRCs). The fibre orientation and the stacking sequence can be opportunely modified in order to achieve the appropriate strength and stiffness (Brischetto, 2014c). The use of CFRCs has been in constant developing in the last thirty years. Their outstanding diffusion in several engineering fields is due to their high performances combined with low weights (high specific properties). Delamination problems and fracture and damage models for multilayered structures have been proposed in Allix et al. (2010), Távara at al. (2010) and Valisetty at al. (2010). Baltacoglu and Civalek (2010), Brischetto (2014a), Brischetto (2014b), Hwu and Yu (2010), Rodríguez-Tembleque and Aliabadi (2014), Yang et al. (2010) and Rodríguez-Tembleque et al. (2013) developed reserved structural models for laminated and sandwich structures. The material property evaluations have been proposed in Buryachenko (2012) and Buryachenko et al. (2012). Prochazka and Valek (2012) proposed the fibre shape optimization. Selvadurai and Nikopour (2012) investigated comparisons between theoretical and experimental results. Typical alternatives to carbon fibre reinforced composites are glass fibre reinforced composites which have the main limitation of a higher mass density (Samborsky et al., 2016; Sanjay et al., 2016; Shah et al., 2013).

Another alternative to typical composites could be natural fibre composites. They are based on renewable resources and they can be used for low cost and eco-friendly structural parts in automotive, aeronautics and space constructions (Kim, 2012). The study of properties, creep resistance, stress relaxation and fatigue of natural fibre composites has become mandatory in the literature (Misra et al., 2011; Carrino and Durante, 2011). Typical natural fibres are linoleum, hemp, flax, sisal, kenaf and jute ones. New studies have been conducted to understand if they could be used as alternative to classical fibres used in polymer composites. Their main advantages are: good mechanical properties, low costs, high specific strength, environmentally-friendly and bio-degradability, ease of fabrication, good structural rigidity and an extensive range of applications (Alkbir et al., 2016). The fundamental disadvantage is their dubious environmental stability (Ansell, 2014). The study of the behavior of natural fibres is fundamental to understand their possible use as reinforcements in composite laminates and sandwiches. Experimental tensile tests for flax fibres were proposed by Baley (2002). Compressive properties of flax, bamboo and coir fibre composites have been investigated by Van Vuure et al. (2015) and Weclawski et al. (2014). Fan and Naughton (2016) studied the thermal decomposition of natural fibre composites using the Dynamic Mechanical Analysis (DMA) as proposed in Saba et. al (2016). An important study about natural fibre composites is the analysis of long-term performances in relation to moisture and other environmental conditions (Hristozov et al., 2015; Summerscales and Grove, 2014). Jauhari et al. (2015) proposed a review concerning physical properties, fabrication methods and failure criteria of natural fibres. The use of natural fibre composites is strictly connected with the concept of eco-design (Le Duigou and Baley, 2014). The works by Pickering et al. (2016) and Pickering and Le (2016) showed the main advantages of natural fibre composites, e.g., low environmental impact, low cost and support for a wide range of applications.

The present work fills the gap present in the literature about the comparison of different structures (plates, cylinders, cylindrical panels and spherical panels) where the laminated and sandwich configurations can include carbon fibre reinforced composites, glass fibre reinforced composites and linoleum fibre reinforced composites. A static analysis is here proposed in analogy to the free vibration analysis already shown in Brischetto (2017c) where the comparison has been performed in terms of frequency values and vibration modes. In this new work, the comparison is proposed in terms of displacements and stresses when a transverse normal load is applied at the top of the structures. The comparisons

are given for different geometries, materials, lamination sequences and thickness ratios. The main scope is to understand if the linoleum fibre composites are comparable, in terms of displacements and stresses, with carbon fibre and glass fibre composites. The employed shell model is a general exact three-dimensional (3D) shell model valid for laminated and sandwich plates, cylinders, cylindrical and spherical shell panels (Brischetto, 2013; Brischetto, 2014a; Brischetto, 2014b; Brischetto, 2016a; Brischetto, 2016b). The closed form solution is obtained using simply supported boundary conditions and harmonic forms for displacements, loads and stresses. The 3D differential equilibrium equations written for spherical shells, using general orthogonal curvilinear coordinates, automatically degenerate in those for plates, cylinders and cylindrical panels employing opportune considerations about radii of curvature. The system is written in layer wise form and it is solved by means of the exponential matrix method (Brischetto et al., 2016b; Tornabene et al., 2015). The developed shell model is a refinement and an advancement of the 3D plate model in orthogonal rectilinear coordinates by Messina (2009), the 3D shell model in cylindrical coordinates by Soldatos and Ye (1995) and the 3D shell model in curvilinear coordinates by Fan and Zhang (1992).

2 Fibre characteristics

In Ashby et al. (2013) and Peek (2008), natural fibres are defined as renewable materials which are recyclable or biodegradable. Composites including natural fibres are also called bio-composites or eco-composites. The possible combinations of matrix and fibres are (BAYDUR, 2016; Bcomp, 2016): - synthetic matrix embedding natural fibres; - renewable synthetic matrix embedding natural fibres; - biodegradable matrix embedding synthetic fibres; - renewable synthetic matrix embedding synthetic fibres; - natural matrix embedding natural fibres. The origin of natural fibres can be vegetable (e.g., cotton, hemp and gaves), animal (e.g., silk and animal pelts) and mineral (e.g., asbestos which is considered very dangerous) (Performance Composites, 2016). The main advantages of natural fibres, in comparison with typical fibres such as carbon and glass ones, are (CW Composites World, 2016): - cheap price; - plentiful availability; - easily available; - no particular respiratory and dermatologist problems; - depending on the employed matrix, the relative eco-composites can be biodegradable, biocompatible and/or recyclable; - the combustion can be used for the transformation process at the end of the material life; - no particularly abrasive; - mass density smaller than that of glass fibres; - mass density similar to that of carbon fibres; - interesting acoustic and thermal insulation properties.

The 3D exact static analysis proposed in the present paper, in analogy with the 3D exact free vibration analysis in Brischetto (2017c), considers composites which include three different fibre types: carbon fibres, glass fibres and linoleum fibres. Carbon fibres are usually included in polymeric matrices (Zoltek, 2016). They have high strength and low weight. They are usually employed in aerospace, automotive, rail transport, maritime transport and sport competition fields. Composites including carbon fibres have a high elastic limit and a high fatigue resistance. Their weight is small and their linear expansion coefficient is low. The corrosion phenomena are not significant and the resistance to chemical compounds is optimal. They have also a good combustion resistance and they could be easily integrated in the structures reducing the number of components. On the contrary, composites including carbon fibers have smaller compression and impact resistance in comparison with metals. They also have problems connected with UAV rays, heat and humidity exposure. A high local damage can be shown if these composites are struck by lightning. Moreover, such composites are not easy to be repaired, they have high costs and they are not recyclable.

A possible classification of glass fibres is made considering their chemical composition and their main properties. E-glass is employed for the electric insulation. Mechanical characteristics of S-glass are higher than those of E-glass. R-glass has excellent mechanical properties, in fact it is usually used in aerospace and aviation fields. D-glass shows low electric losses. AR-glass is usually a reinforcement of the cement (Cristaldi, 2012). C-glass is usually employed for external applications. Glass fibres are

mainly used in the fields concerning aeronautics, automotive, nautical science, wind energy and sport competitions. They have a cheap price and a high speed production. The resistance is significant and the rigidity is appropriate. Thermal and chemical resistances are good. The properties are preserved in several environment conditions because of a low hygrometric sensitivity and an optimal electric insulation. Some possible disadvantages are the presence of a self-abrasion which reduces their resistance and a low fatigue resistance. Mass density of glass fibres is bigger than that of carbon and natural fibres. Their Young modulus is smaller than that of carbon fibres.

The 70% of a linoleum fibre is composed by the cellulose. These fibres are environmentally friendly with low production cost and low weight. The specific properties are competitive and they are recyclable. On the contrary, the quality of these fibres is not homogeneous, and they show some difficulties for the connections. They are particularly sensitive for the hygrometric point of view. The adhesion matrix-fibres is not always optimal. Linoleum fibres are used in the sport competitions for the production of skies, snowboards, skateboards, bikes and aquatic equipments, for the production of structural panels, in particular in the automotive field (Lotus Car, 2016), for the production of musical instruments, for sustainable products and for the reduction of vibrations when they are combined with carbon fibres.

The fibre reinforced composite materials employed for the benchmarks proposed in the present paper (using different geometries and several lamination sequences) are a carbon fibre reinforced composite, a glass fiber reinforced composite and a linoleum fibre reinforced composite. The properties of the carbon fibre composite (see Composite Materials Handbook (2002)) are: Young modulus $E_1 = 113.6GPa$ and $E_2 = E_3 = 9.650GPa$, Poisson ratio $\nu_{12} = 0.334$, $\nu_{13} = 0.328$ and $\nu_{23} = 0.490$, shear modulus $G_{12} = 6.000GPa$, $G_{13} = 6.000GPa$ and $G_{23} = 3.100GPa$. The elastic properties of the glass fibre composite, as shown in Samborsky et al. (2016), are: Young modulus $E_1 = 44.60GPa$, $E_2 = 17.00GPa$ and $E_3 = 16.70GPa$, Poisson ratio $\nu_{12} = 0.262$, $\nu_{13} = 0.264$ and $\nu_{23} = 0.350$, shear modulus $G_{12} = 3.490GPa$, $G_{13} = 3.770GPa$ and $G_{23} = 3.460GPa$. The employed linoleum fibre composite has the elastic properties as shown in Hosseini et al. (2015): Young modulus $E_1 = 28.75GPa$, $E_2 = 4.310GPa$ and $E_3 = 4.290GPa$, Poisson ratio $\nu_{12} = 0.370$, $\nu_{13} = 0.360$ and $\nu_{23} = 0.480$, shear modulus $G_{12} = 2.210GPa$, $G_{13} = 2.230GPa$ and $G_{23} = 1.490GPa$.

From the proposed data, the superiority of the carbon fibre composite is clearly shown. If we consider the mass density (which allows the definition of the specific properties dividing the elastic properties for this quantity), the carbon fibre composite remains the material with the best performances. The mass densities are $\rho = 1265kg/m^3$ for the carbon fibre composite, $\rho = 1900kg/m^3$ for the glass fibre composite and $\rho = 1100kg/m^3$ for the linoleum fibre composite. Considering the elastic properties and the specific elastic properties, the carbon fibre composite remains superior if compared with the linoleum fibre composite (these two materials have a similar mass density). The elastic properties of the glass fibre composite are in general superior than those of the linoleum fibre composite. However, if we consider the specific elastic properties, the performances of the linoleum fibre composite become comparable with those of the glass fibre composite because the linoleum fibre composite is lighter than the glass fibre composite ($\rho = 1100kg/m^3$ vs. $\rho = 1900kg/m^3$).

In order to better understand these features, the static analysis proposed in Section 4 is fundamental because these three composites are compared when they are embedded in different laminated and sandwich configurations and in several geometries (plates, cylinders, cylindrical panels and spherical panels).

3 Exact three-dimensional shell model

The employed 3D shell model uses the three-dimensional equilibrium equations based on the general orthogonal curvilinear coordinates α, β and z:

$$H_\beta\frac{\partial\sigma^k_{\alpha\alpha}}{\partial\alpha}+H_\alpha\frac{\partial\sigma^k_{\alpha\beta}}{\partial\beta}+H_\alpha H_\beta\frac{\partial\sigma^k_{\alpha z}}{\partial z}+(\frac{2H_\beta}{R_\alpha}+\frac{H_\alpha}{R_\beta})\sigma^k_{\alpha z}=0\,, \tag{1}$$

$$H_\beta\frac{\partial\sigma^k_{\alpha\beta}}{\partial\alpha}+H_\alpha\frac{\partial\sigma^k_{\beta\beta}}{\partial\beta}+H_\alpha H_\beta\frac{\partial\sigma^k_{\beta z}}{\partial z}+(\frac{2H_\alpha}{R_\beta}+\frac{H_\beta}{R_\alpha})\sigma^k_{\beta z}=0\,, \tag{2}$$

$$H_\beta\frac{\partial\sigma^k_{\alpha z}}{\partial\alpha}+H_\alpha\frac{\partial\sigma^k_{\beta z}}{\partial\beta}+H_\alpha H_\beta\frac{\partial\sigma^k_{zz}}{\partial z}-\frac{H_\beta}{R_\alpha}\sigma^k_{\alpha\alpha}-\frac{H_\alpha}{R_\beta}\sigma^k_{\beta\beta}+(\frac{H_\beta}{R_\alpha}+\frac{H_\alpha}{R_\beta})\sigma^k_{zz}=0\,, \tag{3}$$

the proposed equations are valid for spherical shells and they degenerate in those for cylinders, cylindrical panels and plates by means of simple considerations about the radii of curvature R_α and/or R_β measured with respect to the mean surface Ω_0. H_α and H_β are the parametric coefficients as detailed in Brischetto (2013). Index k is used for the physical layers and it goes from 1 to the total number of layers N_L. The partial derivatives are indicated by means of ∂ and the six stress components are $\boldsymbol{\sigma}^k=\{\sigma^k_{\alpha\alpha}\,\sigma^k_{\beta\beta}\,\sigma^k_{zz}\,\sigma^k_{\beta z}\,\sigma^k_{\alpha z}\,\sigma^k_{\alpha\beta}\}^T$.

Constitutive equations $\boldsymbol{\sigma}^k=\boldsymbol{C}^k\boldsymbol{\epsilon}^k$, geometrical relations $\boldsymbol{\epsilon}^k=\boldsymbol{\Delta}^k\boldsymbol{u}^k$ and harmonic forms for displacements and stresses are substituted in Eqs.(1)-(3) in order to obtain their explicit closed form. Strain vector is $\boldsymbol{\epsilon}^k=\{\epsilon^k_{\alpha\alpha}\,\epsilon^k_{\beta\beta}\,\epsilon^k_{zz}\,\gamma^k_{\beta z}\,\gamma^k_{\alpha z}\,\gamma^k_{\alpha\beta}\}^T$ and displacement vector is $\boldsymbol{u}^k=\{u^k\,v^k\,w^k\}^T$. The meaning of the matrix $\boldsymbol{C}^k$ of the elastic coefficients in the structural reference system (for orthotropic angle equals 0° or 90°) and the meaning of the matrix $\boldsymbol{\Delta}^k$ (containing the differential operators and the geometrical terms) have been given in details in several past author's works (Brischetto, 2013; Brischetto, 2014a; Brischetto, 2014b). The closed form of Eqs.(1)-(3) is proposed using the index j in place of the index k in order to introduce several mathematical layers to calculate constant parametric coefficients H_α and H_β through the thickness direction z:

$$\begin{aligned}&\Big(-\frac{C^j_{55}H^j_\beta}{H^j_\alpha R^2_\alpha}-\frac{C^j_{55}}{R_\alpha R_\beta}-\bar\alpha^2\frac{C^j_{11}H^j_\beta}{H^j_\alpha}-\bar\beta^2\frac{C^j_{66}H^j_\alpha}{H^j_\beta}\Big)U^j+\Big(-\bar\alpha\bar\beta C^j_{12}-\bar\alpha\bar\beta C^j_{66}\Big)V^j+\\&\Big(\bar\alpha\frac{C^j_{11}H^j_\beta}{H^j_\alpha R_\alpha}+\bar\alpha\frac{C^j_{12}}{R_\beta}+\bar\alpha\frac{C^j_{55}H^j_\beta}{H^j_\alpha R_\alpha}+\bar\alpha\frac{C^j_{55}}{R_\beta}\Big)W^j+\Big(\frac{C^j_{55}H^j_\beta}{R_\alpha}+\frac{C^j_{55}H^j_\alpha}{R_\beta}\Big)U^j_{,z}+\Big(\bar\alpha C^j_{13}H^j_\beta+\\&\bar\alpha C^j_{55}H^j_\beta\Big)W^j_{,z}+\Big(C^j_{55}H^j_\alpha H^j_\beta)U^j_{,zz}=0\,,\end{aligned} \tag{4}$$

$$\begin{aligned}&\Big(-\bar\alpha\bar\beta C^j_{66}-\bar\alpha\bar\beta C^j_{12}\Big)U^j+\Big(-\frac{C^j_{44}H^j_\alpha}{H^j_\beta R^2_\beta}-\frac{C^j_{44}}{R_\alpha R_\beta}-\bar\alpha^2\frac{C^j_{66}H^j_\beta}{H^j_\alpha}-\bar\beta^2\frac{C^j_{22}H^j_\alpha}{H^j_\beta}\Big)V^j+\\&\Big(\bar\beta\frac{C^j_{44}H^j_\alpha}{H^j_\beta R_\beta}+\bar\beta\frac{C^j_{44}}{R_\alpha}+\bar\beta\frac{C^j_{22}H^j_\alpha}{H^j_\beta R_\beta}+\bar\beta\frac{C^j_{12}}{R_\alpha}\Big)W^j+\Big(\frac{C^j_{44}H^j_\alpha}{R_\beta}+\frac{C^j_{44}H^j_\beta}{R_\alpha}\Big)V^j_{,z}+\Big(\bar\beta C^j_{44}H^j_\alpha+\\&\bar\beta C^j_{23}H^j_\alpha\Big)W^j_{,z}+\Big(C^j_{44}H^j_\alpha H^j_\beta)V^j_{,zz}=0\,,\end{aligned} \tag{5}$$

$$\begin{aligned}&\Big(\bar\alpha\frac{C^j_{55}H^j_\beta}{H^j_\alpha R_\alpha}-\bar\alpha\frac{C^j_{13}}{R_\beta}+\bar\alpha\frac{C^j_{11}H^j_\beta}{H^j_\alpha R_\alpha}+\bar\alpha\frac{C^j_{12}}{R_\beta}\Big)U^j+\Big(\bar\beta\frac{C^j_{44}H^j_\alpha}{H^j_\beta R_\beta}-\bar\beta\frac{C^j_{23}}{R_\alpha}+\bar\beta\frac{C^j_{22}H^j_\alpha}{H^j_\beta R_\beta}+\bar\beta\frac{C^j_{12}}{R_\alpha}\Big)V^j+\\&\Big(\frac{C^j_{13}}{R_\alpha R_\beta}+\frac{C^j_{23}}{R_\alpha R_\beta}-\frac{C^j_{11}H^j_\beta}{H^j_\alpha R^2_\alpha}-\frac{2C^j_{12}}{R_\alpha R_\beta}-\frac{C^j_{22}H^j_\alpha}{H^j_\beta R^2_\beta}-\bar\alpha^2\frac{C^j_{55}H^j_\beta}{H^j_\alpha}-\bar\beta^2\frac{C^j_{44}H^j_\alpha}{H^j_\beta}\Big)W^j+\end{aligned} \tag{6}$$

$$\Big(-\bar{\alpha} C^j_{55} H^j_\beta - \bar{\alpha} C^j_{13} H^j_\beta \Big) U^j_{,z} + \Big(-\bar{\beta} C^j_{44} H^j_\alpha - \bar{\beta} C^j_{23} H^j_\alpha \Big) V^j_{,z} + \Big(\frac{C^j_{33} H^j_\beta}{R_\alpha} + \frac{C^j_{33} H^j_\alpha}{R_\beta} \Big) W^j_{,z} +$$
$$\Big(C^j_{33} H^j_\alpha H^j_\beta \Big) W^j_{,zz} = 0 \, .$$

Eqs.(4)-(6) assemble a system of three second order partial differential relations in z. The coefficients are constant, even if shell geometries are considered, because of the use of the j mathematical layers. Terms $\bar{\alpha}$ and $\bar{\beta}$ are $\frac{m\pi}{a}$ and $\frac{n\pi}{b}$, respectively. a and b are the shell dimensions. m and n are the half-wave numbers. Eqs.(4)-(6) are written in compact form simply redoubling the number of variables:

$$\boldsymbol{D}^j \frac{\partial \boldsymbol{U}^j}{\partial \tilde{z}} = \boldsymbol{A}^j \boldsymbol{U}^j \, , \tag{7}$$

where $\frac{\partial \boldsymbol{U}^j}{\partial \tilde{z}} = \boldsymbol{U}^{j\prime}$ and $\boldsymbol{U}^j = [U^j \; V^j \; W^j \; U^{j\prime} \; V^{j\prime} \; W^{j\prime}]$. Coordinate $\tilde{z}$ goes from 0 at the bottom to h at the top. The system of differential equations in (7) is solved by means of the exponential matrix method:

$$\boldsymbol{D}^j \boldsymbol{U}^{j\prime} = \boldsymbol{A}^j \boldsymbol{U}^j \, , \tag{8}$$
$$\boldsymbol{U}^{j\prime} = \boldsymbol{D}^{j-1} \boldsymbol{A}^j \; \boldsymbol{U}^j \, , \tag{9}$$
$$\boldsymbol{U}^{j\prime} = \boldsymbol{A}^{j*} \; \boldsymbol{U}^j \, , \tag{10}$$

with $\boldsymbol{A}^{j*} = \boldsymbol{D}^{j-1} \boldsymbol{A}^j$. Matrices $\boldsymbol{D}^j$, $\boldsymbol{A}^j$ and $\boldsymbol{A}^{j*}$ have constant terms in each j layer of the structure. Therefore, the solution can be written as:

$$\boldsymbol{U}^j(\tilde{z}^j) = exp(\boldsymbol{A}^{j*} \tilde{z}^j) \boldsymbol{U}^j(0) \quad \text{with} \quad \tilde{z}^j \, \epsilon \, [0, h^j] \, , \tag{11}$$

$\tilde{z}^j$ is the coordinate through the thickness of each j layer (its values are 0 at the bottom and h^j at the top). The exponential matrix can be developed using $\tilde{z}^j = h^j$ for each j mathematical layer:

$$\boldsymbol{A}^{j**} = exp(\boldsymbol{A}^{j*} h^j) = \boldsymbol{I} + \boldsymbol{A}^{j*} \, h^j + \frac{\boldsymbol{A}^{j*2}}{2!} {h^j}^2 + \frac{\boldsymbol{A}^{j*3}}{3!} {h^j}^3 + \ldots + \frac{\boldsymbol{A}^{j*N}}{N!} {h^j}^N \, , \tag{12}$$

$\boldsymbol{I}$ is the 6×6 identity matrix. The method uses a layer-wise approach. Therefore, interlaminar continuity for displacements (compatibility conditions) and for transverse normal/shear stresses (equilibrium conditions) are imposed as:

$$u^j_b = u^{j-1}_t \, , \;\; v^j_b = v^{j-1}_t \, , \;\; w^j_b = w^{j-1}_t \, , \tag{13}$$
$$\sigma^j_{zzb} = \sigma^{j-1}_{zzt} \, , \;\; \sigma^j_{\alpha zb} = \sigma^{j-1}_{\alpha zt} \, , \;\; \sigma^j_{\beta zb} = \sigma^{j-1}_{\beta zt} \, , \tag{14}$$

each component at the top (t) of the j-1 layer must be equal to the relative component at the bottom (b) of the j layer. The final algebraic system to be solved is:

$$\boldsymbol{E} \quad \boldsymbol{U}^1(0) \;\; = \;\; \boldsymbol{P} \;\; , \tag{15}$$

where the 6×1 unknown vector $\boldsymbol{U}^1(0)$ and the load vector $\boldsymbol{P}$ are:

$$\boldsymbol{U}^1(0) \;\; = \begin{bmatrix} U^1(0) \\ V^1(0) \\ W^1(0) \\ U^{1\prime}(0) \\ V^{1\prime}(0) \\ W^{1\prime}(0) \end{bmatrix} \, , \qquad \boldsymbol{P} \;\; = \begin{bmatrix} P^M_{zt} \\ 0 \\ 0 \\ 0 \\ 0 \\ 0 \end{bmatrix} \, . \tag{16}$$

The vector $\boldsymbol{U}^1(0)$ includes the three displacement components calculated at the bottom of the first layer and the relative derivatives made with respect to the z coordinate. The vector $\boldsymbol{P}$ contains the loads which can be applied at the external surfaces. In the proposed benchmark, the case with a transverse normal load P_z applied at the top (t) of the last layer M is considered. The solution uses a layer-wise approach. The matrix $\boldsymbol{E}$ has always 6×6 dimension for each employed number of mathematical layers M. The general solution has been developed in an in-house academic software, using a Matlab environment, called *3DES*. The model and the code have been extensively validated and tested in several past author's works, in particular in Brischetto (2017a) for the static analysis of sandwich and laminated plates and shells, and in Brischetto (2017b) for the static analysis of functionally graded structures. In both works, comparisons with other 3D solutions in the literature and new benchmarks have been proposed. In Brischetto (2017a) and Brischetto (2017b), it has been demonstrated how M=300 mathematical layers and order N=3 for the exponential matrix are always sufficient for a correct analysis. These values will be used with confidence for the results proposed in the next section.

4 Results

The proposed benchmarks, employed to compare the carbon fibre composite, the glass fibre composite and the linoleum fibre composite, are based on four different geometries. All the proposed structures are simply supported and subjected to an harmonic transverse normal load applied at the top surface with amplitude $P_z = 10000Pa$. The imposed half wave numbers are always $m = n = 1$. Only the cylinder has the circumferential half-wave number $m = 2$ and the axial half-wave number $n = 1$. The first geometry is a square plate with in-plane dimensions $a = b = 1m$ and thickness ratios $a/h = 10$ and $a/h = 50$ (h is the total thickness). The second geometry is a cylinder with dimensions $a = 2\pi R_\alpha$ and $b = 20m$, radii of curvature $R_\alpha = 10m$ and $R_\beta = \infty$, and thickness ratios $R_\alpha/h = 10$ and $R_\alpha/h = 100$. The third geometry is a cylindrical shell panel with dimensions $a = \frac{\pi}{3}R_\alpha$ and $b = 20m$, radii of curvature $R_\alpha = 10m$ and $R_\beta = \infty$, and thickness ratios $R_\alpha/h = 10$ and $R_\alpha/h = 100$. The last geometry is a spherical shell panel with dimensions $a = b = \frac{\pi}{3}R_\alpha$, radii of curvature $R_\alpha = R_\beta = 10m$, and thickness ratios $R_\alpha/h = 10$ and $R_\alpha/h = 100$.

The four employed benchmarks are explicitly proposed in Figure 1. The first benchmark (B1) considers a square sandwich plate with an internal soft core with thickness $h_3 = 0.8h$ and two external composite skins. The bottom composite skin is made of two composite layers with thickness $h_1 = h_2 = 0.05h$ and lamination sequence $90°/0°$. The top composite skin is made of two composite layers with thickness $h_4 = h_5 = 0.05h$ and lamination sequence $0°/90°$. The soft core is isotropic and it has Young modulus $E = 180MPa$ and Poisson ratio $\nu = 0.37$. The laminated skins can be in carbon fibre reinforced composite, glass fibre reinforced composite and linoleum fibre reinforced composite. All these properties have already been given in Section 2. The second benchmark (B2) considers a three-layered laminated cylinder with thickness values $h_1 = h_2 = h_3 = h/3$ and lamination sequence $0°/90°/0°$. The same three different fibre reinforced composites have been used. The third benchmark (B3) is a four layered cylindrical shell panel where the laminae can be made of carbon fibre reinforced composite, glass fibre reinforced composite or linoleum fibre reinforced composite. The thickness values are $h_1 = h_2 = h_3 = h_4 = h/4$ and the lamination sequence is $0°/90°/0°/90°$. The last benchmark (B4) is a sandwich spherical shell panel with the same soft core already employed in the Benchmark 1. The thickness of the soft core is $h_3 = 0.8h$. The bottom composite skin has lamination sequence $90°/0°$ and the bottom composite skin has the same lamination sequence $90°/0°$. The thickness values are $h_1 = h_2 = h_4 = h_5 = 0.05h$. The laminae in the composite skins can be made of the fibre reinforced composites already presented in Section 2.

Figure 2 shows the transverse displacement w in meters through the thickness direction of the four proposed benchmarks in the case of transverse normal load applied at the top ($P_z = 10000Pa$). Moderately thick structures are considered with $a/h = 10$ and $R_\alpha/h = 10$. Results in black color are

for the cases of Carbon Fibre (CF) reinforced composites, red lines are for the cases of Glass Fibre (GF) reinforced composites and green color results are for the use of Linoleum Fibre (LF) reinforced composites. The results for the Carbon Fibre cases are the more rigid ones. Results for Linoleum Fibre cases are comparable with those for the Glass Fibre reinforcements, in particular if we consider that the mass density of the Linoleum Fibre reinforced composite is approximately the half value of that for the Glass Fibre reinforced composite (e.g., the values are $\rho = 1100kg/m^3$ vs. $\rho = 1900kg/m^3$ in the proposed benchmarks). In terms of transverse displacement, when the applied loads are not particularly severe, the Linoleum Fibre reinforced composite can substitute the Glass Fibre reinforced composite. Only for particular conditions, the Linoleum Fibre reinforced composite can even substitute the Carbon Fibre reinforced composite.

The same benchmarks are also proposed in details in Tables 1-4 giving the three displacement components in meters and the six stress components in Pascal through different thickness positions. For each table, moderately thick and thin structures are investigated. Table 1 proposes displacements and stresses for the benchmark 1 about the sandwich square plate with external composite skins. Results are proposed at the top, at the middle and at the top of the structure. The superiority of the Carbon Fibre reinforced composite is clearly shown. The Linoleum Fibre reinforced composite is comparable with the Glass Fibre reinforced composite, in particular if we consider the low value of the mass density for this natural composite. Similar conclusions can be obtained from the Table 2 about the benchmark 2 regarding the three-layered composite cylinder. Table 3 is about the four-layered composite cylindrical shell panel. In this case, two different values are given for the results at the middle surface because this surface coincides with the interface between the second and the third layer. $z = 0^-$ indicates the top of the second layer and $z = 0^+$ indicates the bottom of the third layer. Displacements and transverse stresses are continuous at this interface because of the compatibility and equilibrium conditions, respectively. In-plane stresses can be discontinuous at this interface. Table 4 gives results for the benchmark 4 about the sandwich spherical shell panel with external composite skins. Displacements and stresses are proposed at the top, at the middle and at the top. In the four benchmarks, the boundary load conditions are always satisfied. In fact, $\sigma_{\alpha z}$ and $\sigma_{\beta z}$ are zero at both top and bottom external surfaces for each benchmark, thickness ratio and material. The transverse normal stress σ_{zz} is equal 10000Pa at the top external surface, and it is equal 0Pa at the bottom external surface. These last boundary load conditions are confirmed for each benchmark, thickness ratio and material. From Tables 1-4, it is clear how the Linoleum Fibre reinforced composite is not in general comparable in terms of displacement values with the Carbon Fibre reinforced composite (they have a similar value for the mass density). On the contrary, the displacements for the Linoleum Fibre reinforced composite are comparable with those for the Glass Fibre reinforced composite. This feature is further confirmed by the mass density of the two composites. The mass density of the Glass Fibre reinforced composite is approximately twice the mass density of the Linoleum Fibre reinforced composite. The displacements obtained with the Glass Fibre reinforced composite are approximately the half of those obtained with the Linoleum Fibre reinforced composite. This last feature means that, in a qualitative sense, a structure including the Linoleum Fibre reinforced composite has approximately the same rigidity of a structure embedding the Glass Fibre reinforced composite if the two elements have approximately the same weight. This last consideration is valid for all the four proposed tables and for different geometries, laminations and thickness ratios. However, this conclusion needs a further confirmation from the theoretical and experimental point of view.

5 Conclusions

The present paper has proposed the comparison in terms of displacements and stresses between different sandwich and laminated plates and shells when subjected to a transverse normal load applied at the top. The sandwich and laminated configurations can include a Carbon Fibre reinforced composite, a

Glass Fibre reinforced composite or a Linoleum Fibre reinforced composite. The idea is to understand if, for particular conditions and for not excessive loads, the natural composites (such as the Linoleum Fibre reinforced composite) can be used in place of Carbon Fibre reinforced composites and/or Glass Fibre reinforced composites. This preliminary study seems to give a positive response for the use of the Linoleum Fibre reinforced composite in place of the Glass Fibre reinforced composite. The comparison with the Carbon Fibre reinforced composite seems much more thorny and it needs further analyses. These considerations have been verified for different geometries (plates, cylinders, cylindrical panels and spherical panels), different laminations (symmetrical or anti-symmetrical laminates and sandwiches) and several thickness ratios (thin and thick structures). The obtained conclusions are in accordance with those already shown in the companion paper about the free vibration analysis of plates and shells including natural and classical composites. The model employed for this preliminary comparative analysis is an exact three-dimensional shell model based on a layer-wise approach and on the exponential matrix solution method.

Bibliography

Alkbir, M.F.M.; Sapuan, S.M.; Nuraini, A.A. and Ishak, M.R. (2016), "Fibre properties and crashworthiness parameters of natural fibre-reinforced composite structure: a literature review", *Composite Structures*, Vol. 148, pp. 59-73.

Allix, O.; Kerfriden, P. and Gosselet, P. (2010), "A relocalization technique for the multiscale computation of delamination in composite structures", *CMES: Computer Modeling in Engineering & Sciences*, Vol. 55 No. 3, pp. 271-292.

Ansell, M.P. (2014), "Natural fibre composites in a marine environment", in Hodzic, A. and Shanks, R. (Ed.), Natural Fibre Composites. Materials, Processes and Applications, Woodhead Publishing Ltd., pp. 365-374.

Ashby, M.; Shercliff, H. and Cebon, D. (2013), Materials: Engineering, Science, Processing and Design, Butterworth-Heinemann, Oxford.

Baley, C. (2002), "Analysis of the flax fibres tensile behaviour and analysis of the tensile stiffness increase", *Composites Part A: Applied Science and Manufacturing*, Vol. 33 No. 7, pp. 939-948.

Baltacoglu, A. and Civalek, O. (2010), "Geometrically nonlinear analysis of anisotropic composite plates resting on nonlinear elastic foundations", *CMES: Computer Modeling in Engineering & Sciences*, Vol. 68 No. 1, pp. 1-24.

BAYDUR Trial Product PU 60BD33 (2017), available at: `http://www.gammapoliuretani.com/wp-content/uploads/2015/12/baydur_60_scheda_tecnica.pdf` (accessed 5 June 2017).

Bcomp natural fibre composites (2017), available at: `http://www.bcomp.ch/` (accessed 5 June 2017).

Brischetto, S. (2013), "Exact elasticity solution for natural frequencies of functionally graded simply-supported structures", *CMES: Computer Modeling in Engineering & Sciences*, Vol. 95 No. 5, pp. 391-430.

Brischetto, S. (2014a), "Three-dimensional exact free vibration analysis of spherical, cylindrical and flat one-layered panels", *Shock and Vibration*, Vol. 2014, pp. 1-29.

Brischetto, S. (2014b), "An exact 3D solution for free vibrations of multilayered cross-ply composite and sandwich plates and shells", *International Journal of Applied Mechanics*, Vol. 6 No. 6, pp. 1-42.

Brischetto, S. (2014c), "Innovative multilayered structures for a new generation of aircraft and spacecraft", *Journal of Aeronautics & Aerospace Engineering*, Vol. 4 No. 1, pp. 1-2.

Brischetto, S. (2016a), "Exact and approximate shell geometry in the free vibration analysis of one-layered and multilayered structures", *International Journal of Mechanical Sciences*, Vol. 113, pp. 81-93.

Brischetto, S. (2016b), "Convergence analysis of the exponential matrix method for the solution of 3D equilibrium equations for free vibration analysis of plates and shells", *Composites: Part B*, Vol. 98,

pp. 453-471.
Brischetto, S. (2017a), "Exact three-dimensional static analysis of single- and multi-layered plates and shells", *Composites: Part B*, Vol. 119, pp. 230-252.
Brischetto, S. (2017b), "A general exact elastic shell solution for bending analysis of functionally graded structures", *Composite Structures*, Vol. 175, pp. 70-85.
Brischetto, S. (2017c), "A comparative study of composite structures including carbon, glass and natural fibers", *Multidiscipline Modeling in Materials and Structures*, in press.
Brischetto, S.; Ciano, A. and Ferro, C.G. (2016a), "A multipurpose modular drone with adjustable arms produced via the FDM additive manufacturing process", *Curved and Layered Structures*, Vol. 3 No. 1, pp. 202-213.
Brischetto, S.; Tornabene, F.; Fantuzzi, N. and Viola, E. (2016b), "3D exact and 2D generalized differential quadrature models for free vibration analysis of functionally graded plates and cylinders", *Meccanica*, Vol. 51 No. 9, pp. 2059-2098.
Buryachenko, V.A. (2012), "Modeling of random bimodal structures of composites (application to solid propellants): II. Estimation of effective elastic moduli", *CMES: Computer Modeling in Engineering & Sciences*, Vol. 85 No. 5, pp. 417-446.
Buryachenko, V.A.; Jackson, T.L. and Amadio, G. (2012), "Modeling of random bimodal structures of composites (application to solid propellants): I. Simulation of random packs", *CMES: Computer Modeling in Engineering & Sciences*, Vol. 85 No. 5, pp. 379-416.
Carrino, L. and Durante, M. (2011), "Realizzazione e Caratterizzazione di Laminati in Composito Polimerico Termoplastico Rinforzato con Fibre Naturali. Produzione di Laminati con Fibre Naturali e loro Caratterizzazione", Research report. Universitá degli Studi di Napoli "Federico II".
Cristaldi, G. (2012), "Sviluppo di Materiali Compositi Rinforzati con Fibre Naturali per l'Ingegenria Civile", Ph.D. Thesis. Universitá degli Studi di Catania.
CW Composites World (2017), available at: `http://www.compositesworld.com/articles/eco-elise-concept-lean-speedy-and-green` (accessed 5 June 2017).
Department of Defense Handbook (2002), "Polymer Matrix Composites Materials. Usage, Design, and Analysis", Composite Materials Handbook Volume 3.
Fan, M. and Naughton, A. (2016), "Mechanisms of thermal decomposition of natural fibre composites", *Composites Part B: Engineering*, Vol. 88, pp. 1-10.
Fan, J.-R. and Zhang, J.-Y. (1992), "Analytical solutions for thick, doubly curved, laminated shells", *Journal of Engineering Mechanics*, Vol. 188 No. 7, pp. 1338-1356.
Ferro, C.G.; Brischetto, S.; Torre, R. and Maggiore, P. (2016), "Characterization of ABS specimens produced via the 3D printing technology for drone structural components", *Curved and Layered Structures*, Vol. 3 No. 1, pp. 172-188.
Hosseini, N.; Javid, S.; Amiri, A.; Ulven, C.; Webster, D.C. and Karami, G. (2015), "Micromechanical viscoelastic analysis of flax fiber reinforced bio-based polyurethane composites", *Journal of Renewable Materials*, Vol. 3 No. 3, pp. 205-215.
Hristozov, D.; Wroblewski, L. and Sadeghian, P. (2015), "Long-term tensile properties of natural fibre-reinforced polymer composites: comparison of flax and glass fibres", *Composites Part B: Engineering*, Vol. 95, pp. 82-95.
Hwu, C. and Yu, M. (2010), "A comprehensive finite element model for tapered composite wing structures", *CMES: Computer Modeling in Engineering & Sciences*, Vol. 67 No. 2, pp. 151-174.
Jauhari, M.; Mishra, R. and Thakur, H. (2015), "Natural fibre reinforced composite laminates: a review", *Materials Today: Proceedings*, Vol. 2 No. 4-5, pp. 2868-2877.
Kim, Y.K. (2012), "Natural fibre composites (NFCs) for construction and automotive industries", in Kozlowski, R. (Ed.), *Handbook of Natural Fibres. Processing and Applications*, Elsevier, New York, NY, pp. 254-279.
Le Duigou, A. and Baley, C. (2014), "Coupled micromechanical analysis and life cycle assessment as

an integrated tool for natural fibre composites development", *Journal of Cleaner Production*, Vol. 83, pp. 61-69.
Lotus Car (2017), available at `http://www.lotuscars.com/` (accessed 5 June 2017).
Messina, A. (2012), "Three-dimensional free vibration analysis of cross-ply laminated rectangular plates through 2D and exact models", *Mechanics of Advanced Materials and Structures* , Vol. 19 No. 4, pp. 250-264.
Misra, M.; Ahankari, S.S.; Mohanty, A.K. and Nga, A.D. (2011), "Creep and fatigue of natural fibre composites", in Zafeiropoulos, N.E. (Ed.), *Interface Engineering of Natural Fibre Composites for Maximum Performance*, Woodhead Publishing, pp. 289-340.
Peek, N. (2008), "Rapid Prototyping of Green Composites", Master Degree Thesis. University of Amsterdam.
Performance Composites (2017), available at `http://www.performance-composites.org/` (accessed 5 June 2017).
Pickering, K.L.; Aruan Efendy, M.G. and Le, T.M. (2016), "A review of recent developments in natural fibre composites and their mechanical performance", *Composites Part A: Applied Science and Manufacturing*, Vol. 83, pp. 98-112.
Pickering, K.L. and Le, T.M. (2012), "High performance aligned short natural fibre - Epoxy composites", *Composites Part B: Engineering*, Vol. 85, pp. 123-129.
Prochazka, P.P. and Valek, M.J. (2012), "Optimal shape of fibers in transmission problem", *CMES: Computer Modeling in Engineering & Sciences*, Vol. 87 No. 3, pp. 207-224.
Rodríguez-Tembleque, L.; Sáez, A. and Buroni, F.C. (2013), "Numerical study of polymer composites in contact", *CMES: Computer Modeling in Engineering & Sciences*, Vol. 96 No. 2, pp. 131-158.
Rodríguez-Tembleque, L. and Aliabadi, M.H. (2014), "Friction and wear modelling in fiber-reinforced composites", *CMES: Computer Modeling in Engineering & Sciences*, Vol. 102 No. 3, pp. 183-210.
Saba, N.; Jawaid, M.; Alothman, O.Y. and Paridah, M.T. (2016), "A review on dynamic mechanical properties of natural fibre reinforced polymer composites", *Construction and Building Materials*, Vol. 106, pp. 149-159.
Samborsky, D.D.; Mandell, J.F. and Agastra, P. (2017), "3D static elastic constants and strength properties of a Glass/Epoxy unidirectional laminate", Composite Technologies Research Group - Montana State University, available at: `http://www.coe.montana.edu/composites/` (accessed 5 June 2017).
Sanjay, M.R.; Arpitha, G.R. and Yogesha, B. (2016), "Study on mechanical properties of natural-glass fibre reinforced polymer hybrid composites: a review", *Materials Today: Proceedings*, Vol. 2 No. 4-5, pp. 2959-2967.
Selvadurai, A.P.S. and Nikopour, H. (2012), "Uniform loading of a cracked layered composite plate: experiments and computational modelling", *CMES: Computer Modeling in Engineering & Sciences*, Vol. 85 No. 3, pp. 279-298.
Shah, D.U.; Schubel, P.J. and Clifford, M.J. (2013), "Can flax replace E-glass in structural composites? A small wind turbine blade case study", *Composites: Part B*, Vol. 52, pp. 172-181.
Soldatos, K.P. and Ye, J. (1995), "Axisymmetric static and dynamic analysis of laminated hollow cylinders composed of monoclinic elastic layers", *Journal of Sound and Vibration*, Vol. 184 No. 2, pp. 245-259.
Summerscales, J. and Grove, S. (2014), "Manufacturing methods for natural fibre composites", in Hodzic, A. and Shanks, R. (Ed.), *Natural Fibre Composites. Materials, Processes and Applications*, Woodhead Publishing, pp. 176-215.
Távara, L.; Mantic, V.; Graciani, E.; Cañas, J. and París, F. (2010), "Analysis of a crack in a thin adhesive layer between orthotropic materials: an application to composite interlaminar fracture toughness test", *CMES: Computer Modeling in Engineering & Sciences*, Vol. 58 No. 3, pp. 247-270.
Tornabene, F.; Brischetto, S.; Fantuzzi, N. and Viola, E. (2015), "Numerical and exact models for free vibration analysis of cylindrical and spherical shell panels", *Composites: Part B*, Vol. 81, pp. 231-250.

Valisetty, R.; Rajendran, A. and Grove, D. (2010), "Mesh effects in predictions of progressive damage in 3D woven composites", *CMES: Computer Modeling in Engineering & Sciences*, Vol. 60 No. 1, pp. 41-72.
Van Vuure, A.W.; Baets, J.; Wouters, K. and Hendrickx, K. (2015), "Compressive properties of natural fibre composites", *Materials Letters*, Vol. 149, pp. 138-140.
Weclawski, B.T.; Fan, M. and Hui, D. (2014), "Compressive behaviour of natural fibre composite", *Composites Part B: Engineering*, Vol. 67, pp. 183-191.
Yang, B.; Ouyang, J.; Jiang, T. and Liu, C. (2010), "Modeling and simulation of fiber reinforced polymer mold filling process by level set method", *CMES: Computer Modeling in Engineering & Sciences*, Vol. 63 No. 3, pp. 191-222.
Zoltek Commercial Carbon Fiber (2017), available at `http://zoltek.com/carbonfiber/` (accessed 5 June 2017).

	a/h=50								
	u $[10^{-3}m]$	v $[10^{-3}m]$	w $[10^{-3}m]$	$\sigma_{\alpha\alpha}$ $[10^4Pa]$	$\sigma_{\beta\beta}$ $[10^4Pa]$	$\sigma_{\alpha\beta}$ $[10^4Pa]$	σ_{zz} $[10^4Pa]$	$\sigma_{\alpha z}$ $[10^4Pa]$	$\sigma_{\beta z}$ $[10^4Pa]$
Carbon fiber (z=-h/2)	0.0652	0.0644	2.4028	-265.52	-2386.8	244.37	0.0000	0.0000	0.0000
Glass fiber (z=-h/2)	0.1150	0.1146	3.9939	-795.70	-1814.8	251.84	0.0000	0.0000	0.0000
Linoleum fiber (z=-h/2)	0.2138	0.2131	7.1292	-404.53	-2074.4	296.38	0.0000	0.0000	0.0000
Carbon fiber (z=0)	0.0001	0.0001	2.4040	0.2881	0.2881	0.0026	0.5002	8.4954	9.1773
Glass fiber (z=0)	0.0001	0.0001	3.9957	0.2845	0.2845	0.0042	0.5002	8.6998	9.0285
Linoleum fiber (z=0)	0.0002	0.0002	7.1330	0.2765	0.2765	0.0079	0.5002	8.6540	9.1845
Carbon fiber (z=+h/2)	-0.0651	-0.0643	2.4031	265.56	2383.1	-243.94	1.0000	0.0000	0.0000
Glass fiber (z=+h/2)	-0.1149	-0.1144	3.9941	794.75	1812.1	-251.42	1.0000	0.0000	0.0000
Linoleum fiber (z=+h/2)	-0.2134	-0.2127	7.1294	404.33	2071.3	-295.86	1.0000	0.0000	0.0000
	a/h=10								
	u $[10^{-5}m]$	v $[10^{-5}m]$	w $[10^{-5}m]$	$\sigma_{\alpha\alpha}$ $[10^4Pa]$	$\sigma_{\beta\beta}$ $[10^4Pa]$	$\sigma_{\alpha\beta}$ $[10^4Pa]$	σ_{zz} $[10^4Pa]$	$\sigma_{\alpha z}$ $[10^4Pa]$	$\sigma_{\beta z}$ $[10^4Pa]$
Carbon fiber (z=-h/2)	0.4217	0.3231	9.0566	-16.209	-120.71	14.038	0.0000	0.0000	0.0000
Glass fiber (z=-h/2)	0.5999	0.5475	10.321	-40.768	-87.396	12.581	0.0000	0.0000	0.0000
Linoleum fiber (z=-h/2)	1.0141	0.9342	12.847	-18.798	-91.335	13.527	0.0000	0.0000	0.0000
Carbon fiber (z=0)	0.0207	0.0216	9.1079	0.2780	0.2776	0.0087	0.5053	1.6722	1.8310
Glass fiber (z=0)	0.0245	0.0251	10.387	0.2746	0.2743	0.0102	0.5052	1.7170	1.8019
Linoleum fiber (z=0)	0.0328	0.0337	12.953	0.2670	0.2666	0.0137	0.5050	1.7166	1.8421
Carbon fiber (z=+h/2)	-0.4136	-0.3132	9.1891	16.365	117.55	-13.699	1.0000	0.0000	0.0000
Glass fiber (z=+h/2)	-0.5839	-0.5304	10.454	40.030	85.072	-12.218	1.0000	0.0000	0.0000
Linoleum fiber (z=+h/2)	-0.9811	-0.8995	12.985	18.674	88.513	-13.057	1.0000	0.0000	0.0000

Table 1: Benchmark 1, displacements and stresses in a sandwich plate with composite skins.

	R_α/h=100								
	u $[10^{-3}m]$	v $[10^{-3}m]$	w $[10^{-3}m]$	$\sigma_{\alpha\alpha}$ $[10^4Pa]$	$\sigma_{\beta\beta}$ $[10^4Pa]$	$\sigma_{\alpha\beta}$ $[10^4Pa]$	σ_{zz} $[10^4Pa]$	$\sigma_{\alpha z}$ $[10^4Pa]$	$\sigma_{\beta z}$ $[10^4Pa]$
Carbon fiber (z=-h/2)	0.7125	-0.0454	0.8348	143.29	10.947	64.413	0.0000	0.0000	0.0000
Glass fiber (z=-h/2)	1.2112	-0.0559	1.4731	124.58	27.374	64.436	0.0000	0.0000	0.0000
Linoleum fiber (z=-h/2)	1.9504	-0.1465	2.4063	138.24	17.584	64.455	0.0000	0.0000	0.0000
Carbon fiber (z=0)	0.7119	-0.0519	0.8343	14.897	97.803	63.975	0.5027	0.0008	0.0108
Glass fiber (z=0)	1.2098	-0.0675	1.4724	50.880	60.741	63.970	0.5008	0.0025	0.0170
Linoleum fiber (z=0)	1.9481	-0.1653	2.4045	24.567	83.944	63.974	0.5021	0.0014	0.0170
Carbon fiber (z=+h/2)	0.7113	-0.0585	0.8338	143.33	13.424	63.542	1.0000	0.0000	0.0000
Glass fiber (z=+h/2)	1.2085	-0.0790	1.4717	125.98	34.040	63.508	1.0000	0.0000	0.0000
Linoleum fiber (z=+h/2)	1.9459	-0.1841	2.4026	138.66	20.645	63.499	1.0000	0.0000	0.0000
	R_α/h=10								
	u $[10^{-5}m]$	v $[10^{-5}m]$	w $[10^{-5}m]$	$\sigma_{\alpha\alpha}$ $[10^4Pa]$	$\sigma_{\beta\beta}$ $[10^4Pa]$	$\sigma_{\alpha\beta}$ $[10^4Pa]$	σ_{zz} $[10^4Pa]$	$\sigma_{\alpha z}$ $[10^4Pa]$	$\sigma_{\beta z}$ $[10^4Pa]$
Carbon fiber (z=-h/2)	7.4256	1.5895	8.6318	14.480	0.1699	7.0988	0.0000	0.0000	0.0000
Glass fiber (z=-h/2)	12.550	0.5239	15.124	12.034	-0.1971	7.0723	0.0000	0.0000	0.0000
Linoleum fiber (z=-h/2)	20.343	0.3302	24.860	13.874	0.5460	7.1388	0.0000	0.0000	0.0000
Carbon fiber (z=0)	7.3555	-0.5019	8.6065	1.7386	9.7077	6.6313	0.5223	0.0127	0.1105
Glass fiber (z=0)	12.412	-0.6442	15.080	5.3157	6.0392	6.5794	0.5063	0.0260	0.1720
Linoleum fiber (z=0)	20.094	-1.5847	24.736	2.7124	8.3467	6.6253	0.5185	0.0168	0.1092
Carbon fiber (z=+h/2)	7.3028	-1.1800	8.5693	14.933	2.7024	6.2084	1.0000	0.0000	0.0000
Glass fiber (z=+h/2)	12.288	-1.8150	15.012	13.549	6.5499	6.1331	1.0000	0.0000	0.0000
Linoleum fiber (z=+h/2)	19.886	-3.5212	24.569	14.541	3.6704	6.1621	1.0000	0.0000	0.0000

Table 2: Benchmark 2, displacements and stresses in a laminated composite cylinder.

	R_α/h=100								
	u $[10^{-3}m]$	v $[10^{-3}m]$	w $[10^{-3}m]$	$\sigma_{\alpha\alpha}$ $[10^4Pa]$	$\sigma_{\beta\beta}$ $[10^4Pa]$	$\sigma_{\alpha\beta}$ $[10^4Pa]$	σ_{zz} $[10^4Pa]$	$\sigma_{\alpha z}$ $[10^4Pa]$	$\sigma_{\beta z}$ $[10^4Pa]$
Carbon fiber (z=-h/2)	2.7350	-0.2795	8.0787	-131.42	38.637	207.21	0.0000	0.0000	0.0000
Glass fiber (z=-h/2)	4.8754	-0.5683	14.273	-121.89	139.60	207.47	0.0000	0.0000	0.0000
Linoleum fiber (z=-h/2)	8.1196	-1.0840	23.965	-88.590	68.472	209.64	0.0000	0.0000	0.0000
Carbon fiber (z=0^-)	2.6271	-0.3428	8.0774	36.615	624.01	185.89	-0.0025	1.6065	0.4521
Glass fiber (z=0^-)	4.6849	-0.6804	14.271	86.649	499.38	185.59	0.0342	1.4924	0.4920
Linoleum fiber (z=0^-)	7.7994	-1.2720	23.959	57.269	595.65	186.42	0.0905	1.3313	0.4386
Carbon fiber (z=0^+)	2.6271	-0.3428	8.0774	242.28	58.842	185.89	-0.0025	1.6065	0.4521
Glass fiber (z=0^+)	4.6849	-0.6804	14.271	147.94	196.47	185.59	0.0342	1.4924	0.4920
Linoleum fiber (z=0^+)	7.7994	-1.2720	23.959	192.30	97.101	186.42	0.0905	1.3313	0.4386
Carbon fiber (z=+h/2)	2.5191	-0.4062	8.0750	71.438	748.95	164.68	1.0000	0.0000	0.0000
Glass fiber (z=+h/2)	4.4944	-0.7924	14.268	193.62	606.11	163.84	1.0000	0.0000	0.0000
Linoleum fiber (z=+h/2)	7.4792	-1.4599	23.951	104.11	698.17	163.33	1.0000	0.0000	0.0000
	R_α/h=10								
	u $[10^{-5}m]$	v $[10^{-5}m]$	w $[10^{-5}m]$	$\sigma_{\alpha\alpha}$ $[10^4Pa]$	$\sigma_{\beta\beta}$ $[10^4Pa]$	$\sigma_{\alpha\beta}$ $[10^4Pa]$	σ_{zz} $[10^4Pa]$	$\sigma_{\alpha z}$ $[10^4Pa]$	$\sigma_{\beta z}$ $[10^4Pa]$
Carbon fiber (z=-h/2)	9.7467	1.0911	23.061	-75.153	-3.7862	11.253	0.0000	0.0000	0.0000
Glass fiber (z=-h/2)	16.892	1.4641	38.370	-60.375	-9.9389	10.874	0.0000	0.0000	0.0000
Linoleum fiber (z=-h/2)	31.106	2.6912	72.463	-65.123	-5.4342	12.676	0.0000	0.0000	0.0000
Carbon fiber (z=0^-)	7.0433	-0.6405	23.090	1.9104	11.856	5.4852	-0.6479	4.0336	1.2062
Glass fiber (z=0^-)	12.121	-1.4390	38.449	4.4451	11.089	5.1383	-0.5940	3.7298	1.2594
Linoleum fiber (z=0^-)	22.159	-2.7903	72.600	3.1251	13.558	5.8423	-0.5547	3.7359	1.2681
Carbon fiber (z=0^+)	7.0433	-0.6405	23.090	22.485	1.2914	5.4852	-0.6479	4.0336	1.2062
Glass fiber (z=0^+)	12.121	-1.4390	38.449	10.369	4.6702	5.1383	-0.5940	3.7298	1.2594
Linoleum fiber (z=0^+)	22.159	-2.7903	72.600	18.384	2.6425	5.8423	-0.5547	3.7359	1.2681
Carbon fiber (z=+h/2)	4.0859	-2.3104	22.897	11.557	45.415	-0.1098	1.0000	0.0000	0.0000
Glass fiber (z=+h/2)	7.2471	-4.3168	38.202	30.854	38.590	-0.3315	1.0000	0.0000	0.0000
Linoleum fiber (z=+h/2)	12.809	-8.1603	71.906	16.628	43.364	-0.7062	1.0000	0.0000	0.0000

Table 3: Benchmark 3, displacements and stresses in a laminated composite cylindrical shell panel.

	R_α/h=100								
	u $[10^{-3}m]$	v $[10^{-3}m]$	w $[10^{-3}m]$	$\sigma_{\alpha\alpha}$ $[10^4Pa]$	$\sigma_{\beta\beta}$ $[10^4Pa]$	$\sigma_{\alpha\beta}$ $[10^4Pa]$	σ_{zz} $[10^4Pa]$	$\sigma_{\alpha z}$ $[10^4Pa]$	$\sigma_{\beta z}$ $[10^4Pa]$
Carbon fiber (z=-h/2)	0.6983	0.6955	2.3724	36.534	338.80	252.13	0.0000	0.0000	0.0000
Glass fiber (z=-h/2)	1.1662	1.1635	4.0041	112.27	259.68	145.15	0.0000	0.0000	0.0000
Linoleum fiber (z=-h/2)	1.7781	1.7713	6.3417	61.377	319.73	236.50	0.0000	0.0000	0.0000
Carbon fiber (z=0)	0.6672	0.6643	2.3710	1.2950	1.3062	2.6241	0.3962	0.1935	0.1936
Glass fiber (z=0)	1.1128	1.1100	4.0013	2.1359	2.1470	4.3808	0.4010	0.1865	0.1866
Linoleum fiber (z=0)	1.6923	1.6855	6.3356	3.8579	3.8849	6.6569	0.4187	0.1610	0.1611
Carbon fiber (z=+h/2)	0.6362	0.6333	2.3692	541.34	60.903	227.37	1.0000	0.0000	0.0000
Glass fiber (z=+h/2)	1.0596	1.0568	3.9978	411.25	181.39	220.48	1.0000	0.0000	0.0000
Linoleum fiber (z=+h/2)	1.6069	1.6000	6.3282	465.60	91.844	211.56	1.0000	0.0000	0.0000
	R_α/h=10								
	u $[10^{-5}m]$	v $[10^{-5}m]$	w $[10^{-5}m]$	$\sigma_{\alpha\alpha}$ $[10^4Pa]$	$\sigma_{\beta\beta}$ $[10^4Pa]$	$\sigma_{\alpha\beta}$ $[10^4Pa]$	σ_{zz} $[10^4Pa]$	$\sigma_{\alpha z}$ $[10^4Pa]$	$\sigma_{\beta z}$ $[10^4Pa]$
Carbon fiber (z=-h/2)	7.0208	6.7644	21.459	0.8058	14.209	26.119	0.0000	0.0000	0.0000
Glass fiber (z=-h/2)	11.408	11.172	34.134	0.1321	2.9276	24.886	0.0000	0.0000	0.0000
Linoleum fiber (z=-h/2)	17.621	17.085	51.468	-0.6096	0.4162	24.221	0.0000	0.0000	0.0000
Carbon fiber (z=0)	6.3988	6.1470	21.692	0.2795	0.2894	0.2472	0.3445	0.3629	0.3654
Glass fiber (z=0)	9.8114	9.5783	34.199	0.3059	0.3151	0.3821	0.2799	0.4900	0.4917
Linoleum fiber (z=0)	14.202	13.670	51.341	0.4039	0.4248	0.5493	0.2418	0.5837	0.5869
Carbon fiber (z=+h/2)	5.5709	5.3077	21.978	59.889	7.7543	18.649	1.0000	0.0000	0.0000
Glass fiber (z=+h/2)	8.0749	7.8321	34.267	48.859	22.668	15.862	1.0000	0.0000	0.0000
Linoleum fiber (z=+h/2)	10.716	10.149	50.990	56.404	12.041	13.175	1.0000	0.0000	0.0000

Table 4: Benchmark 4, displacements and stresses in a sandwich spherical shell panel with composite skins.

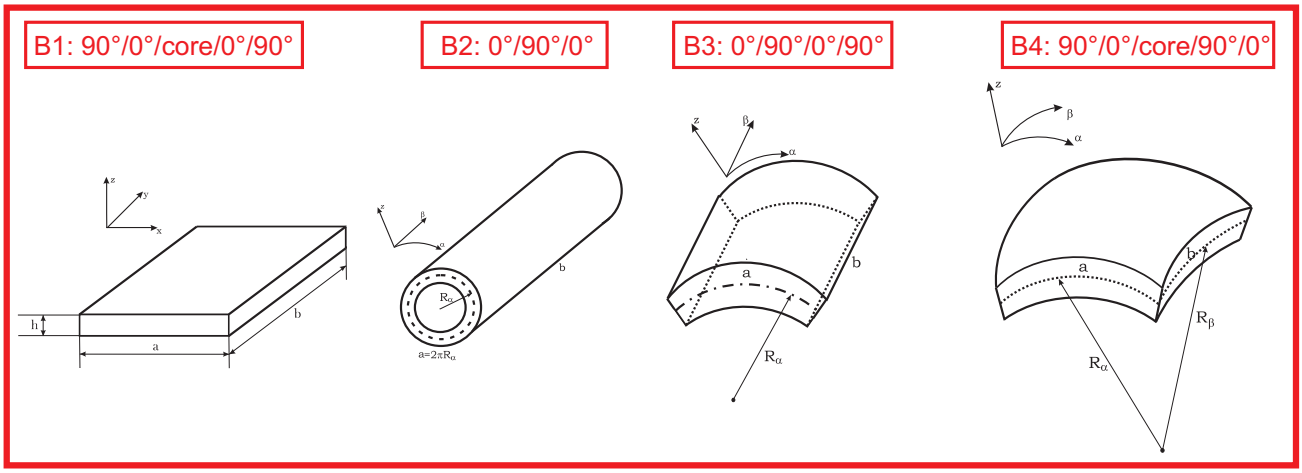

Figure 1: Geometry and lamination sequence for the four proposed benchmarks.

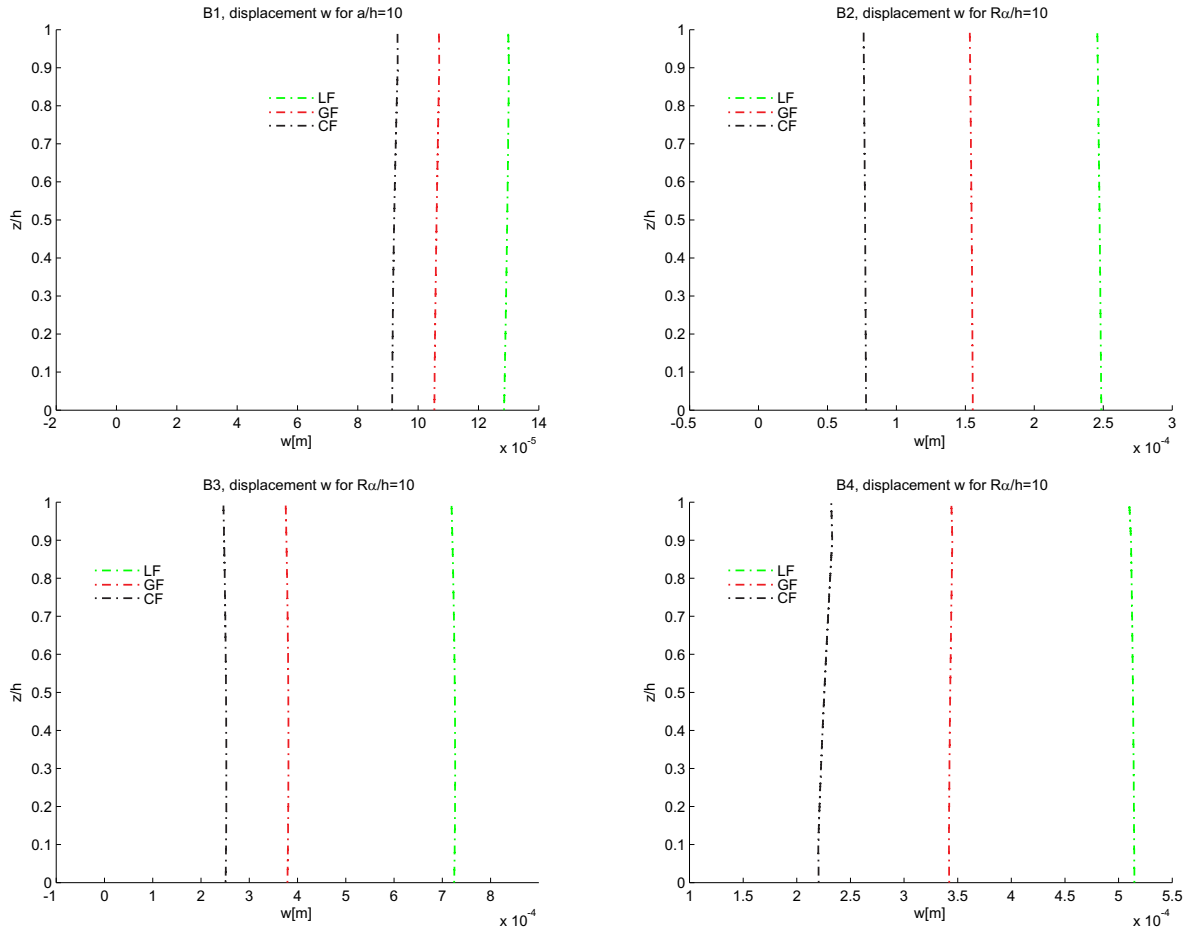

Figure 2: Transverse displacement w through the thickness of plates and shells for different types of reinforcement. CF: Carbon fibre; GF: Glass fibre; LF: Linoleum fibre.